Surface Shortwave Radiation Measurements: Experimental Tests and Numerical Simulations of Pyranometers

M. Haeffelin, A. M. Smith, and J. R. Mahan
Virginia Polytechnic Institute and State University
Blacksburg, Virginia

C. K. Rutledge
Analytical Services and Materials, Inc.
Hampton, Virginia

S. Kato
Hampton University
Hampton, Virginia

Introduction

Pyranometers are used extensively in networks around the globe to monitor solar radiation. Uncertainties in irradiances measured by pyranometers are due in part to the detector sensitivity to thermal radiation exchange within the instrument, often referred to as "instrument offset." Bush et al. (1999) established a relationship between the outer-dome-to-body temperature difference and the instrument offset at night and presented possible corrections for the daytime offsets. Alberta and Charlock (1999) and Dutton et al. (1999) presented adjustments to diffuse shortwave (SW) irradiances measured by shaded pyranometers to reduce negative offsets. These adjustments are based on a relationship derived at night between the net longwave (LW) fluxes at the surface and pyranometer outputs.

To determine the uncertainty in the solar irradiance measured by Eppley's Precision Spectral Pyranometer (PSP) instruments, we propose to better characterize the thermal exchanges in the optical front-end of the instrument through a combination of analytical, experimental, and numerical modeling efforts. Initial experimental work involves high-level calibration of thermistors, determination of optical and thermo-physical properties of the sensors, installation of thermistors in the instrument, and calibration of this modified PSP. An analytical formulation computes the thermal contribution to the PSP signal based on measured temperatures within the instrument. The numerical model will allow us to perform sensitivity studies of the instrument properties as well as to simulate instrument-operating conditions during field measurements. This paper presents the outline of our approach and progress.

Experimental Work

YSI 44031 thermistors are used to measure the temperatures on the inner dome and at the cold junction of the thermopile of the PSP. The thermistors are tested in a calibration bath controlled to ± 0.005 °C. Temperatures determined using YSI standard coefficients show biases ranging from 0.1 °C to 0.2 °C. New Hart-Steinhart coefficients are derived using nine calibration bath temperatures. The root mean square (rms) error of the temperatures is reduced to 0.01 °C.

Knowing the temperature of the hemispherical dome is critical to characterizing the thermal radiation exchange within the instrument. The dome is made of Schott glass and is predominantly transparent to solar radiation. The thermistors are coated with a black paint and, as such, are good absorbers of solar radiation. To optimize the measurement of the dome temperature, the absorption of solar radiation by the thermistor should be minimized and the thermal conductivity between the dome and the thermistor should be maximized.

A PSP glass dome mounted on a slab of wood is used to test coatings and thermally conductive bonding materials. A black thermistor is installed in the center of the hemispherical dome. A second thermistor, coated with white glossy paint, is located in the center as well. These thermistors are only in contact with the air under the dome. A third thermistor is coated with a glossy white paint and bonded to the dome using a thermally conductive white silicon paste.

The dome is initially covered by a box to prevent exposure to solar radiation and allow the thermistors to reach an equilibrium temperature. Once the three thermistors reach the same temperature, the box is removed and the dome is exposed to global solar radiation. After 15 minutes, the direct solar beam is shaded and the dome is only exposed to diffuse solar radiation. The sequence of covered-global-shaded is then repeated several times, with each phase lasting approximately 15 minutes.

Figure 1 shows one particular sequence. At the end of phase 1 (covered), the three thermistors are within 0.2 °C of each other. After the cover is removed and the dome is exposed to solar radiation, the temperature of the three thermistors increase exponentially, a characteristic response to absorption of radiative energy. In the center, the black thermistor is more than 1 °C warmer than the white one at all times. The white thermistor bonded to the glass responds to radiation, as evidenced by the initial exponential increase, but this temperature increase is limited by its thermal bonding to the dome.

To further investigate the response of the thermistors to solar radiation, we successively shade and unshade each of the three thermistors described earlier in intervals of five minutes. We use a small shading device to limit the shaded area to the cross-sectional area of the thermistors. Figure 2 reveals no evidence that shading solar radiation has a direct effect on the temperature of the thermistor bonded to the dome. However, the black and the white thermistors in the center of the dome drop in temperature, by 2 °C and 1 °C, respectively, when they are shaded from the direct sunlight. The temperature increase is of the same order when the thermistors are unshaded.
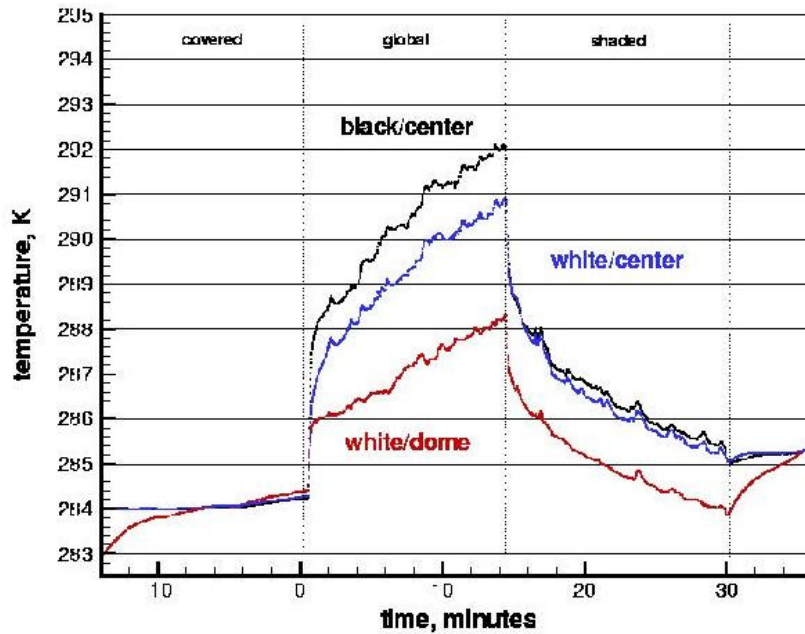
Figure 1.   Measured temperatures from three thermistors on an isolated pyranometer outside dome. Two thermistors are located in the center of the dome and one is in thermal contact with the dome. The dome is successively covered, exposed to global solar radiation and shaded from direct solar radiation.
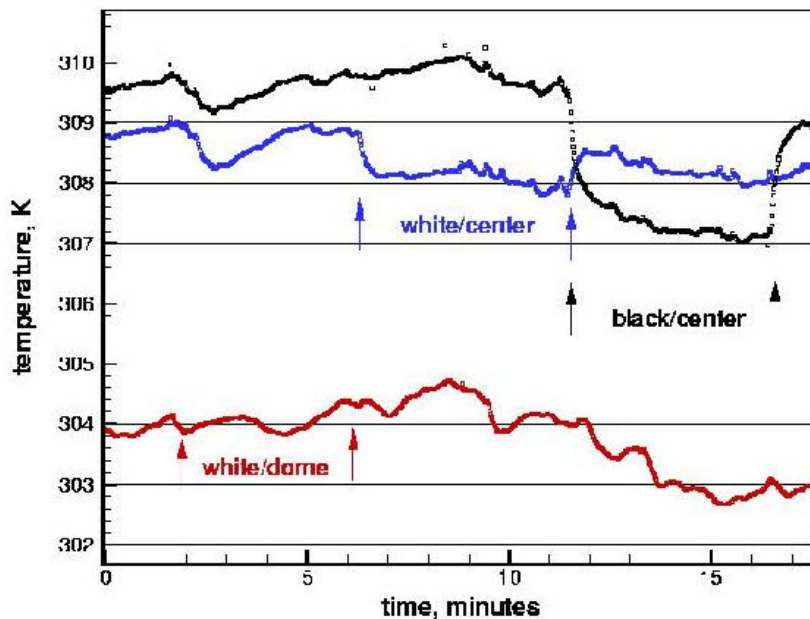
Figure 2. Thermistor temperatures as each thermistor is successively shaded for a five-minute period from direct solar radiation and then unshaded. The area shaded is limited to the cross-sectional area of the thermistor.

Finally, to isolate the response to direct solar radiation from natural temperature fluctuations, we produce a sequence of shading and unshading cycles of higher frequency. The thermistor bonded to the dome is shaded and unshaded for periods of ten seconds. Figure 3 shows that the resulting temperature oscillations are on the order of 0.2 °C. This level of response to solar radiation is satisfactory. We are currently investigating further reduction of the radiation absorption by using thermistors with smaller cross-sectional areas.
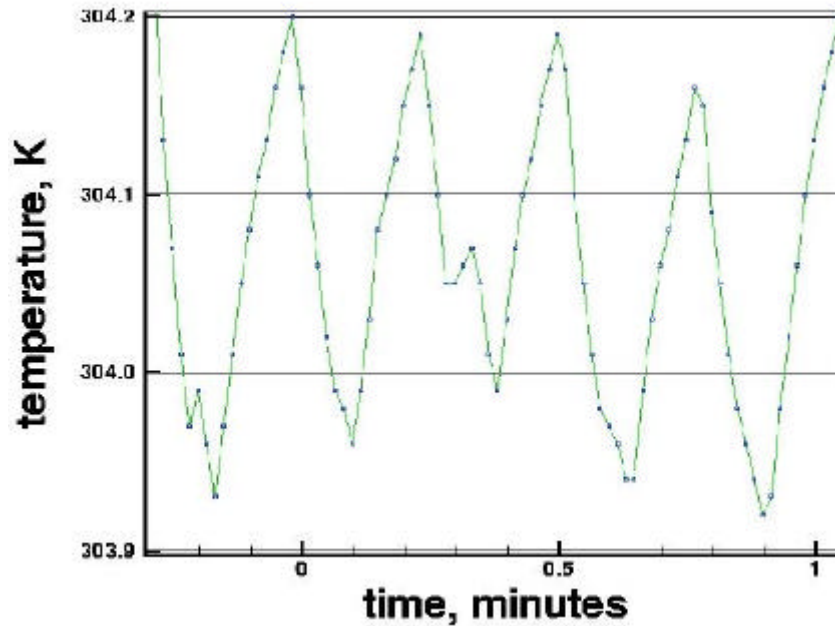

Figure 3. Thermistor temperature of the white thermistor bonded to the dome as it is shaded and unshaded in ten-second intervals. The small amplitude of the oscillation indicates that the effect of direct solar radiation on the thermistor temperature is not significant.

Analytical Model

We developed an analytical model of the energy balance of the pyranometer to relate measured instrument temperatures to instrument offsets. This model is inspired from analyses carried out for the pyrgeometer instrument by Albrecht et al. (1974), Philipona et al. (1995), and Fairwall et al. (1998). The temperature gradient through a thermopile is a function of the net absorbed radiation at the sensor surface, $F_{net} = (T_s - T_b)/c$, where T_s and T_b are the hot and cold junction temperatures, respectively, and c is the sensitivity in K/Wm^{-2}. As depicted in Figure 4, F_{net} can also be defined as

$$F_{net} = \alpha_s \tau_d E + \alpha_s \varepsilon_d \sigma T_d^{\ 4} + \alpha_s \varepsilon_s \rho_d \sigma T_s^{\ 4} - \varepsilon_s \sigma T_s^{\ 4}, \tag{1}$$
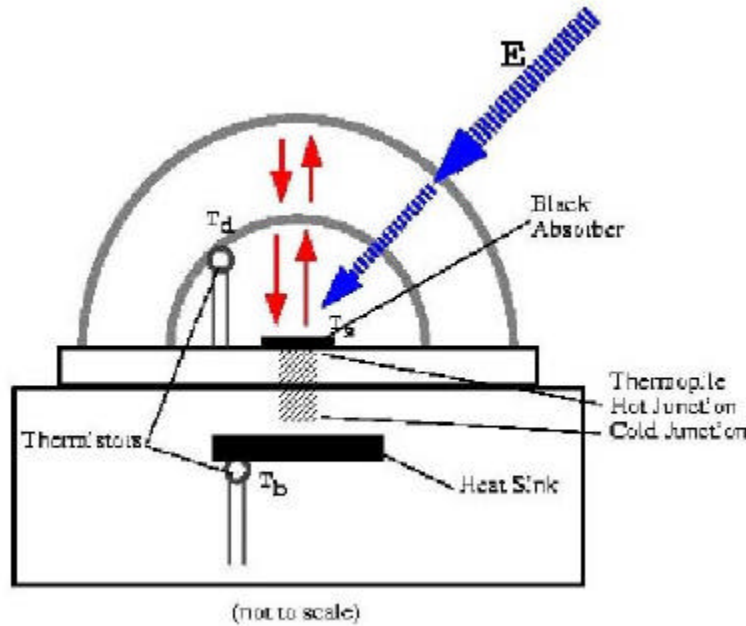
Figure 4. Schematic diagram of the key components of a pyranometer. The large dashed arrows represent downwelling solar radiation and the solid arrows the thermal radiation exchanged within the instrument.

where α_s and ε_s are the absorptivity and emissivity of the sensor, τ_d is the transmissivity of the dome in the solar spectral domain, ε_d and ρ_d are the emissivity and reflectivity of the dome, T_d is the effective temperature of the dome, and E is the incoming solar irradiance. A voltage, U_e, proportional to the temperature gradient is generated. We solve for E and rewrite Eq. (1) in terms of the measurable quantities U_e, T_b, and T_d,

$$E = U_e \left[\frac{S}{\alpha_s \tau_d c} + \frac{4\sigma S}{\tau_d} (1 - \varepsilon_s \rho_d) T_b^{\,3} \right] + \frac{\varepsilon_d \sigma}{\tau_d} (\varepsilon_s T_b^{\,4} - T_d^{\,4}) + \frac{\sigma}{\tau_d} (1 - \alpha_s) T_b^{\,4}, \qquad (2)$$

where S is the Seebeck coefficient of the thermopile. The first term on the right side of Eq. (2) contains two terms within the bracket, which represent the proportionality between the thermopile output voltage and the downwelling solar irradiance. The first term in the bracket is the effect of solar irradiance, whereas the second term accounts for the radiative effect of the temperature increase of the hot junction due to absorption of solar irradiance. The second term modifies the slope between E and U_e by about 2.5%. Both terms are accounted for in calibration. However, the temperature dependence of the slope associated with the $T_b^{\,3}$ term remains. The other two terms of Eq. (2) represent the amount of irradiance, which must be accounted for to compensate the radiative exchange, which takes place between the inner dome and the detector. The two terms add up to more than 15 Wm^{-2} when the inner dome is 3 °C cooler than the instrument body at 20 °C. Bush et al. (1999) have shown that 15 Wm^{-2} offsets are obtained when the outer dome is just 4 °C cooler than the instrument body.

If the operating temperature of the pyranometer remains close to the calibration temperature Eq. (2) can be parameterized as

$$E = KU_e + C_1(\varepsilon_s T_b{}^4 - T_d{}^4) + C_2 T_b{}^4, \tag{3}$$

K is determined through calibration and C_1 and C_2 are derived from nighttime observations. Thermistor sondes will be installed initially in two Eppley pyranometers. The pyranometers will be calibrated according to the standard Baseline Surface Radiation Network procedures. The instruments will be submitted to conditions, which create large temperature gradients between the dome and the body, in the absence of any solar radiation (E=0). Coefficient C_1 and C_2 can be determined experimentally by varying the operating conditions through a large range of temperatures. The same coefficients are used to compute the correct irradiance during daytime.

Numerical Model

In a parallel effort, we built a finite-element numerical model to simulate the heat transfer between the components of the pyranometer. A numerical approximation is used in order to characterize the complex geometry. Such a numerical model can accurately represent transient conductive, convective, and radiative heat exchanges between all elements of the instrument. The instrument is defined geometrically with a finite-element mesh. Each element is defined by a series of nodes at which the solution to the heat transfer problem are computed. The elements can have different shapes and sizes to best represent the actual instrument geometry. Boundary conditions, such as constant or variable temperatures or surface heat flux, are specified for the entire domain. For example, solar radiative input on the instrument is represented as a surface heat flux on the dome; it can be combined with both thermal radiative and convective heat exchange between the dome and the surrounding environment. The different source and sink terms can be turned on and off independently to determine their individual impact. This high-level numerical model will allow us to better understand simple energy exchange within the instrument as well as to simulate the real conditions under which the instrument operates during field measurements. Figure 5 shows an example of the geometry and the steady-state temperature distribution in the instrument submitted to radiative cooling to a cold sky and convective heating by surrounding air.

One important issue is that we are not able to verify experimentally is the offsets computed for daytime measurements. The model will allow us to compute offsets for both nighttime and daytime conditions and to check whether an empirical relation derived in the absence of solar radiation can be applied to derive daytime offset corrections. The accuracy of the model is limited only by the accuracy of our knowledge of thermophysical properties of the materials used in the pyranometer as well as our ability to represent detailed geometry of the assembly. To determine accurate thermophysical properties, which are not well known, we perform parameter studies using the model and compare the results to experimental data obtained from simple and well-defined operating conditions, such as the illumination of the instrument by a calibrated radiation source.
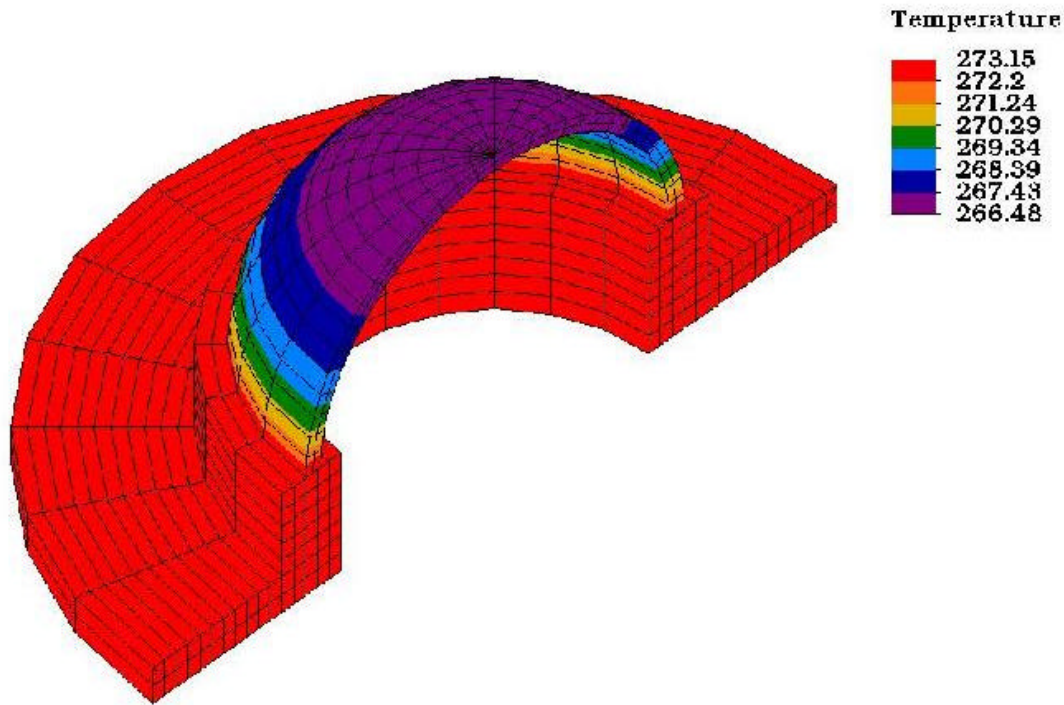
Figure 5. Finite element grid of the instrument geometry and temperature distribution resulting from radiative cooling to clear sky and convective heating to ambient air.

We initially develop a finite-element numerical model using a commercial software package. The commercial package enables us to quickly develop a realistic representation of a pyranometer. A code developed in-house will be more flexible in terms of simulating realistic conditions where conduction, convection, and radiative heat transfer modes are combined in transient conditions. We performed a sensitivity study of the effect of convective heat exchange between the dome and the surrounding air on the dome temperature at night. The study shows that the temperature gradient from the base of the dome to its tip, which, in the absence of wind, can be as high as 10 °C under clear-sky conditions at night. This gradient is reduced to about 3 °C with a sustained 10 m/s wind convecting air at ambient temperature uniformly over the dome (heat transfer coefficient h=40 $Wm^{-2}K^{-1}$). Figure 6 depicts the temperature gradient from the base of the dome to the tip for different boundary conditions. Increased wind speed can significantly reduce the gradient, however the convective heating cannot completely compensate the radiative cooling. This simulation shows that ventilation of the dome can reduce the thermal gradient across the outside dome, a condition, which should also reduce instrument offset. This example highlights the necessity in our experimental tests to operate both ventilated and unventilated instruments in the field and compare the instrument offsets in both configurations.

Summary and Future Work

We demonstrate our ability to measure PSP dome temperatures. We develop an analytical model to derive offset corrections from measured instrument temperatures. We also develop a numerical tool to support the experimental work.
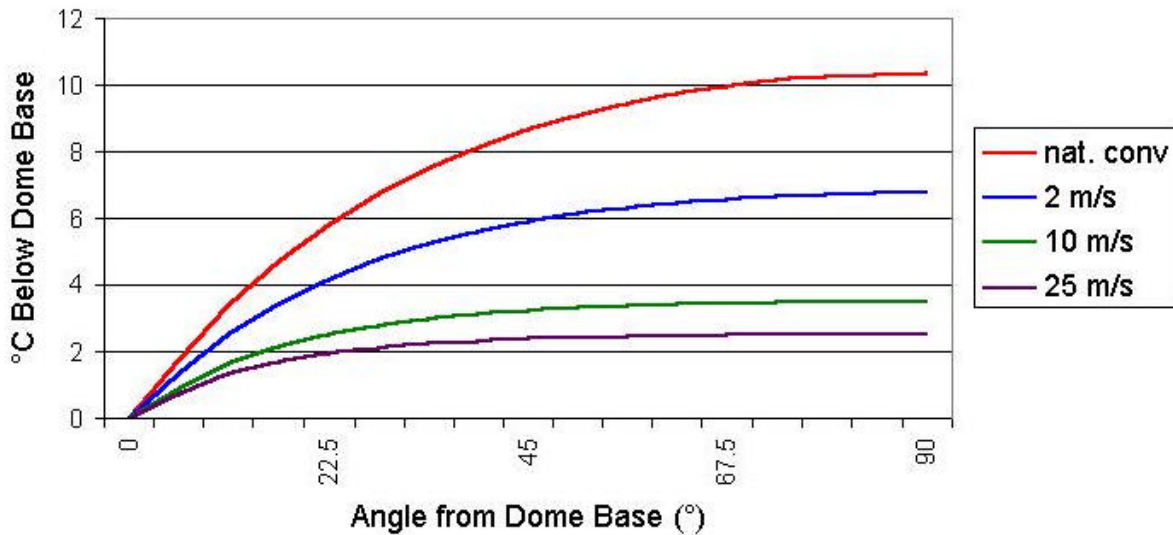
Figure 6. Temperature gradients across the dome (base to tip) for different conditions of convection (no wind to 25m/s wind). The dome cools radiatively to a cold clear sky (brightness temperature 220K). The temperature of the ambient air is 273K. The wind has a heating effect which partially compensates the radiative cooling.

We are currently installing thermistors in several pyranometers. The pyranometers will be calibrated after modification. Laboratory tests will be conducted to derive the parameters of the analytical model relating instrument temperatures to offsets. Field tests will be conducted to monitor instrument offsets through a range of operating conditions. The numerical model will be used to verify that the parameters to the analytical model derived in laboratory, in the absence of solar radiation, can be applied to derive offsets in the field, under solar radiation.

References

Alberta, T. L., and T. P. Charlock, 1999: A comprehensive resource for the investigation of the shortwave fluxes in clear conditions: CAGEX V3. Preprint of the 10th Conference on Atmospheric Radiation. AMS, Boston, Massachusetts.

Albrecht, B., M. Peollet, and S. K. Cox, 1974: Pyrgeometer measurements from aircraft. *Rev. Sci. Instrum*., **45**, 33-38.

Bush, B. C., F. P. J. Valero, A. S. Simpson, and L. Bignone, 1999: Characterization of thermal effects in pyranometers: A data correction algorithm for improved measurement of surface insolation. *J. Atmos. Res. and Ocean. Tech.* In press.

Dutton, E. G., T. Stoffel, and J. J. Michalsky, 1999: Measurement of broadband diffuse solar irradiance: Error sources and corrections. This proceedings.

Fairall, C. W., P. O. G. Persson, E. F. Bradley, R. E. Payne, and S. P. Anderson, 1998: A new look at calibration and use of Eppley precision infrared radiometers. Part I: Theory and application. *J. Atmos. Ocean. Tech.*, **15**, 1229-1242.

Philipona, R., C. Frohlich, and Ch. Betz, 1995: Characterization of pyrgeometers and the accuracy of atmospheric long-wave radiation measurements. *Applied Optics*, **34**, 1598-1605.